Measurement of Large Spiral and Target Waves in Chemical Reaction-Diffusion-Advection Systems: Turbulent Diffusion Enhances Pattern Formation

A. von Kameke,* F. Huhn, A. P. Muñuzuri, and V. Pérez-Muñuzuri

Group of Nonlinear Physics, University of Santiago de Compostela, E-15782 Santiago de Compostela, Spain

(Received 13 September 2012; published 20 February 2013)

In the absence of advection, reaction-diffusion systems are able to organize into spatiotemporal patterns, in particular spiral and target waves. Whenever advection is present that can be parametrized in terms of effective or turbulent diffusion D_*, these patterns should be attainable on a much greater, boosted length scale. However, so far, experimental evidence of these boosted patterns in a turbulent flow was lacking. Here, we report the first experimental observation of boosted target and spiral patterns in an excitable chemical reaction in a quasi-two-dimensional turbulent flow. The wave patterns observed are ~50 times larger than in the case of molecular diffusion only. We vary the turbulent diffusion coefficient D_* of the flow and find that the fundamental Fisher-Kolmogorov-Petrovsky-Piskunov equation, $v_f \propto \sqrt{D_*}$, for the asymptotic speed of a reactive wave remains valid. However, not all measures of the boosted wave scale with D_* as expected from molecular diffusion, since the wave fronts turn out to be highly filamentous.

DOI: 10.1103/PhysRevLett.110.088302 PACS numbers: 82.40.Ck, 47.27.tb, 47.54.Fj

Pattern formation in reaction-diffusion-advection (RDA) systems is an important process in many natural and man-made systems, e.g., plankton growth and iron fertilization in the ocean [1], dispersion of pollutants in the atmosphere, and optimal mixing in chemical reactors [2]. Spiral and target waves have been observed on small scales in various active media, e.g., in chicken retina [3], cardiac tissue [4], or chemical reactions [5,6]. From a geophysical viewpoint it is of crucial interest if these reaction-diffusion patterns can also be found in large scale systems involving turbulent advection, as, for example, plankton dynamics in the ocean affecting CO_2 absorption [1,2,7]. Theoretically, the appearance of spiral and target waves should be possible in RDA systems whenever the advection term can be parametrized as a global diffusion coefficient [8]. However, so far, experimental evidence of these patterns in turbulent flows is lacking. Despite the importance of pattern formation in RDA systems only very few laboratory experiments on turbulent fluid flow involve reaction kinetics [9], and to our knowledge, none has considered excitable kinetics so far. Considerable numerical and experimental effort has focused on cellular and chaotic flows [2,10–12]. However, in those flows the derivation of a global diffusion coefficient seems to be more involved than in turbulent flows [12], and thus the propagation of reactive waves is likely to depend on the details of the flow [10]. In this Letter, we show experimentally that pattern formation, in particular, spiral and target waves can occur in turbulent fluid flows and we find that the front expansion is governed by the Fisher-Kolmogorov-Petrovsky-Piskunov (FKPP) equation.

We create a quasi-two-dimensional turbulent flow using the Faraday experiment [13,14]; i.e., we vertically vibrate a circular container of 30 cm diameter filled with 2 mm of an excitable cyclohexanedione and ferroin based Belousov-Zhabotinsky reaction [14,15] (see Supplemental Material for methods summary and supplementary Fig. S1 [16]). The dynamics of this chemical reaction can be well observed with a camera in the visible range due to the oxidation of the reddish catalyst ferroin $[Fe(phen)_3^{2+}]$ to the blue ferriin $[Fe(phen)_3^{3+}]$ [17]. We vary the intensity of the turbulence and thus the turbulent diffusion constant [12] D_* by altering the amplitude a_0 of the acceleration and the frequency f of the vertical forcing.

In Fig. 1 we present examples of boosted spiral and target waves in the turbulent flow. The upper panel, 1–3, shows an image sequence of a spontaneous boosted spiral and the lower panel, 1–3, a spontaneous boosted target wave (Supplemental Material, movies $M1$ and $M2$ [16]). Without any fluid flow the much smaller usual target and spiral patterns of a pure reaction-diffusion system can be observed. They are shown for comparison on the right (image 4). The boosted patterns are a very robust phenomenon and were found for a large range of forcing parameters, $f = 30$–140 Hz, $a_0 = 0.6$–$2.5g$, g being the gravitational constant. The temporal persistence of the target patterns varies from some minutes for high forcing amplitudes a_0, to up to one hour for lower ones. The probability for a target to form is higher for lower forcing. This is most likely related to more long-lived structures in the fluid flow [18] that favor the occurrence of a perturbation that is persistent and big enough to trigger a new wave [19]. Usually, but not always, target waves are triggered at the border of the container. Spiral waves form spontaneously, most often created by the breakup of target waves due to interactions with the turbulent fluid flow or the boundary. Figure 1 (upper panel, image 2) shows the trajectory of a spiral tip in time. The temporal persistence of the spiral is

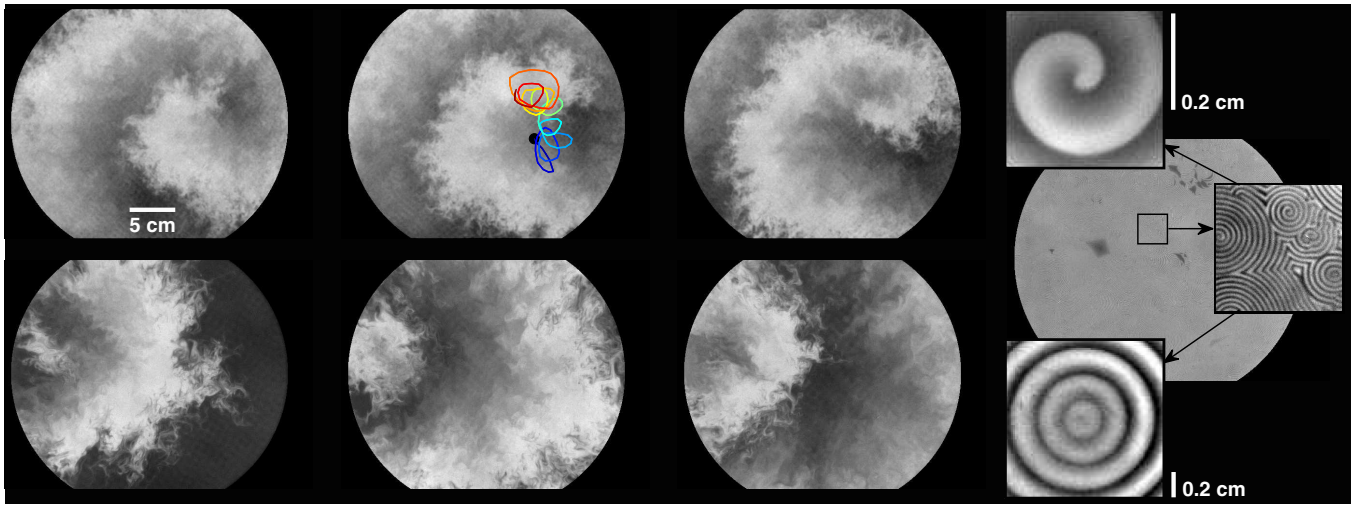

FIG. 1 (color online). Boosted spiral and target patterns of an excitable chemical Belousov-Zhabotinsky reaction in a turbulent flow. Grey scale indicates concentration of ferriin, $Fe(phen)_3^{3+}$. Upper panel, 1–3: Image sequence of boosted spiral with $\Delta t \approx 3.6$ s, $f = 70$ Hz, $a_0 \approx 1.8g$, $[H_2SO_4] = 1.2$ M. 2nd image: Trajectory of spiral tip in time (color code: early position blue, late position red). Lower panel, 1–3: Image sequence of boosted target wave with $\Delta t \approx 12.4$ s, $f = 50$ Hz, $a_0 \approx 1.2g$, $[H_2SO_4] = 0.6$ M. Both patterns form spontaneously and are persistent phenomena that can last from a few minutes up to one hour. For corresponding movies ($M1$, $M2$) see Supplemental Material [16]. Right: Three close-ups show molecular-diffusion-induced spiral and target patterns in absence of fluid flow in the same container. Note the large difference in scales between these usual and the boosted patterns.

limited due to the complex movement of the tip [20,21] since it eventually hits the border or another pattern, causing the spiral to vanish (Supplemental Material, movies $M1$ and $M3$ [16]). If, in contrast, we prevent the spiral to drift by pinning its tip to a round obstacle of 54 mm diameter, placed in the middle of the container, spirals last for up to ~1 h (see Supplemental Material, movies $M4$, $M5$, and $M6$ [16]).

For a quantitative analysis of the rotation periods of the boosted spirals we varied the turbulent diffusion of the flow. This was achieved by changing only the forcing amplitude a_0 leaving the forcing frequency, and thus the Faraday wavelength λ_F constant [13,22] ($f = 50$ Hz, $[H_2SO_4] = 0.6$ M, Supplemental Material, example movie $M3$ [16]). However, the periods of the boosted spirals at $f = 50$ Hz are all in the same range of $T = 30$–50 s for all forcings with only a slight tendency towards longer periods for stronger forcings. This might be explained by the augmentation of the width of the boosted autowaves such that the spirals seem to be restricted by their own tail [20]. This self-restriction could also explain why the period of the molecular-diffusion-induced spiral, $T_{\mathrm{mol}} = 18$–25 s, was somewhat lower. In addition to the spiral and target patterns, we also observe double spirals with two free curling ends, another typical pattern known from reaction-diffusion systems [2] (Supplemental Material, movie $M7$ [16]). All reactive waves had the typical characteristics of autowaves, in particular, they annihilate when they meet.

In reaction-diffusion systems the front velocity v_f of travelling waves can most often be described by the FKPP relation, i.e., $v_f = 2\sqrt{D_*/\tau_{\mathrm{reac}}}$ [2,8,23]. The front velocity v_f is thus simply given by the only two parameters determining the dynamics of the reaction-diffusion system, namely, the typical time scale τ_{reac} of the reaction and the diffusion constant D_*. The solid line in Figs. 2(a) and inset 2(b) represents the FKPP prediction from the molecular diffusion case extended to larger values of the diffusion constant. The reaction time scale for our chemical reaction was estimated to be $\tau_{\mathrm{reac}} = (0.8 \pm 0.3)$ s from inserting the measured velocity of the molecular-diffusion-induced target wave into the FKPP relation and using a molecular diffusion coefficient reported in the literature, $D_{\mathrm{mol}} \approx (1.3$–$2.0) \times 10^{-3}$ mm^2/s [19,24,25]. We find that the FKPP relation remains valid for well developed boosted target waves in the quasi-two-dimensional turbulent flow, see Figs. 2(a) and inset 2(b). Surprisingly, the front velocities v_f of the boosted target waves agree with the prediction derived from the FKPP equation using only measurements from experiments with molecular diffusion. Front velocity measurements v_f were taken as a mean of at least two different realizations of the experiment and more than 15 different target waves at constant forcing. The front velocity of each target wave was measured by averaging over the intensity of an image stripe along the direction of front propagation and the successive determination of the spatial evolution of the minimal first spatial derivative of the signal in time (Fig. S3, Supplemental Material [16]).

Theoretically, when the reaction time scale is small in comparison to the time scale of the fluid flow, the front velocity v_f is bounded by the unidirectional root-mean-square velocity of the flow instead of obeying the FKPP

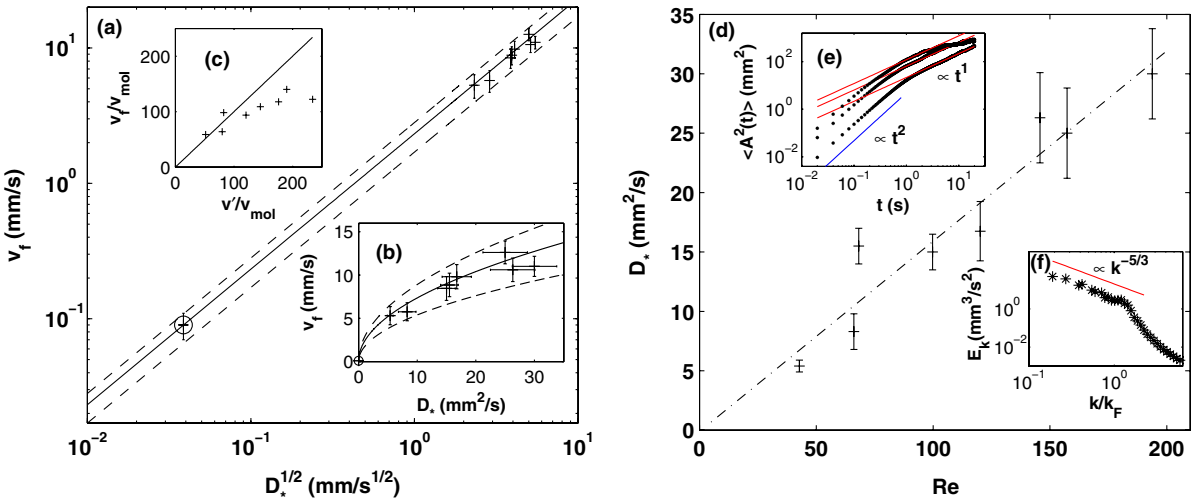

FIG. 2 (color online). Front velocity of reactive waves in dependence of turbulent diffusion. (a) The velocity of the boosted target wave fronts v_f (crosses) follows the FKPP prediction $v_f = 2\sqrt{D_*/\tau_{\mathrm{reac}}}$ (solid line) derived from the molecular case (circle). Dashed lines indicate the error bounds estimated from the standard deviation of the velocity measurements from the molecular-diffusion-induced target wave. Inset (b) shows a close up of the turbulent data pairs. (c) Target front velocity v_f vs turbulent root-mean-square velocity of the turbulent flow in one direction $v' = v_{\mathrm{rms}}/\sqrt{2}$, both normalized to the front velocity v_{mol} of the molecular-diffusion-induced target wave. (d) The measured diffusion coefficients are shown as a function of the Reynolds number $\mathrm{Re} = v_{\mathrm{rms}}\lambda_F/\nu$ indicating the turbulence strength, where ν is the kinematic viscosity of the fluid. Inset (e) shows the absolute diffusion for the flows with $\mathrm{Re} \approx 43$, $\mathrm{Re} \approx 120$, and $\mathrm{Re} \approx 194$ and the linear fit for estimation of the turbulent diffusion coefficient. Inset (f) shows an exemplary energy spectrum of the flow for $\mathrm{Re} \approx 120$. A double cascade and a regime with a Kolmogorov type scaling ($E_k \propto k^{-5/3}$) can be distinguished. k_F is the typical Faraday wave number.

relation [26]. Inset Fig. 2(c) shows that in our experiments this limit is only approached for low forcing.

In Fig. 2(d), diffusive transport in the turbulent flow is characterized. The measured turbulent diffusion coefficient D_* is plotted as a function of the estimated Reynolds number for different forcing amplitudes. The turbulent diffusion increases approximately linearly with the Reynolds number as expected. At these Reynolds numbers, the flow is turbulent as can be seen in an exemplary energy spectrum ($\mathrm{Re} \approx 120$) revealing a double cascade and a Kolmogorov type scaling ($\propto k^{-5/3}$) in inset Fig. 2(f) [9,14,27]. The turbulent diffusion coefficients D_* were estimated from measurements of the absolute dispersion $\langle A^2(t)\rangle = \langle|\vec{x}_i(t) - \vec{x}_i(t=0)|^2\rangle = 4D_* t$ [Fig. 2(e)], by a fit to the regime of linear growth. $\vec{x}_i(t)$ is the position of particle i at time t.

Despite the validity of the FKPP prediction for the front speed, Fig. 3 demonstrates that the boosted target waves do not entirely behave like their molecular diffusion counterparts. An important difference is the complex filamentous structure of the reaction front which is related to the small scale stretching and folding processes in the turbulent dynamics [Fig. 3(a), 3(b), and 1] [9,26,28]. For smaller turbulent diffusion [Fig. 3(a)], the filamentary structure increases due to two distinct processes. First, the increase of the length and persistence of the filaments can be explained by an increase of coherent flow structures for lower forcings, i.e., more long-lived eddies and jets, that order the flow on time scales longer than the reaction time τ_{reac}. An imprint of the filaments can be seen in the ferriin concentration profiles [Fig. 3(c)]. The peaks of high concentration ahead of the front show the intermittency of the turbulent diffusion process on these spatiotemporal scales. For stronger turbulent forcing, the fronts are less intermittent [Fig. 3(d)]. Second, the sharper and more pronounced appearance of the filaments can be explained by the Damköhler number, $\mathrm{Da} = \tau_{\mathrm{flow}}/\tau_{\mathrm{reac}}$, the ratio of the typical time scales of the flow and the reaction. As a flow time scale we use the ratio of the Faraday wavelength and the root-mean-square flow velocity, $\tau_{\mathrm{flow}} = \lambda_f/v_{\mathrm{rms}}$. Da varied from $\mathrm{Da} \approx 0.4$ for the highest forcing to $\mathrm{Da} \approx 1.8$ for the lowest (Supplemental Material, Fig. S2 [16]). For small Da, i.e., strong forcing, the fluid flow is fast compared to the reaction time scale which causes the front to be smoother. For large Da, and thus lower forcing, the front appears sharper and its velocity approaches the root mean square velocity of the flow in one direction, $v' = v_{\mathrm{rms}}/\sqrt{2}$ [26,28]. This limit is reached in our experiments for small forcings as is reflected by inset (c) in Fig. 2.

Figures 3(a) and 3(b), show further properties of the target autowaves in the two extreme cases of the measured turbulent diffusion. Differences can be observed in the wave front velocities, as well as in the frequencies of spontaneous wave formation and in the widths of the wave front. In order to quantify this dependence of the widths of the wave front on the turbulent diffusion,

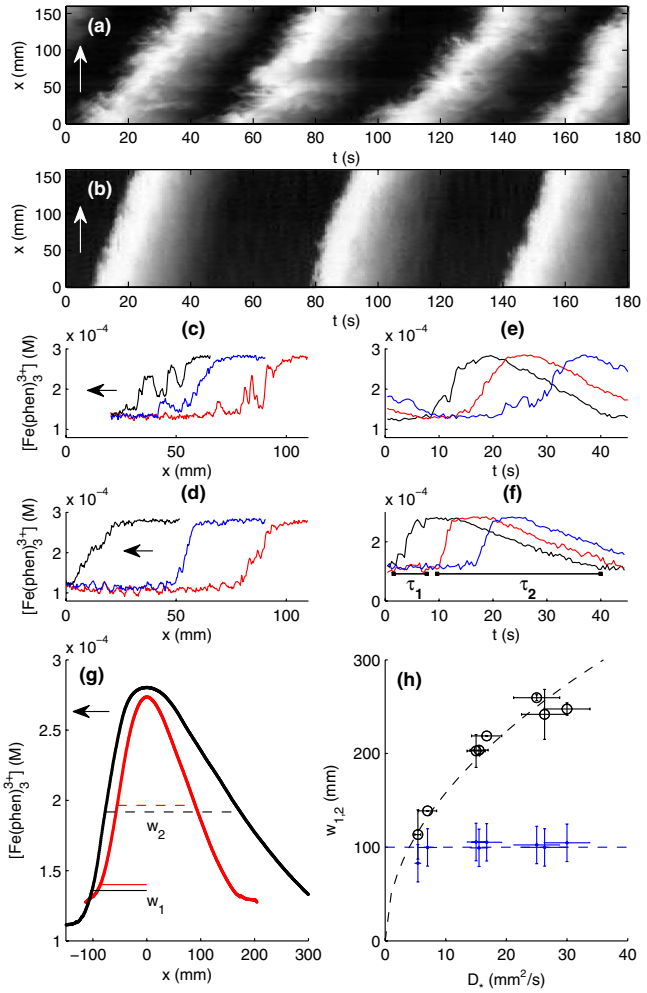

FIG. 3 (color online). Front characteristics of boosted target waves. (a), (b) Space-time plots of boosted targets for $D_* \approx 5.4$ mm^2/s ($a \approx 1.3 g_0$) and $D_* \approx 30.0$ mm^2/s ($a \approx 2.2 g_0$). Arrows indicate the direction of front propagation (Supplemental Material movies $M2$ and $M8$ [16]). The target waves are narrower, slower, and more filamentous for the smaller diffusion coefficient. (c), (d) Ferriin concentration, [Fe(phen)$_3^{3+}$], along a line at three different instances of time, $\Delta t \approx 6.4$ s, for $D_* \approx 5.4$ mm^2/s and $D_* \approx 30.0$ mm^2/s respectively. (e), (f) Ferriin concentrations in time for the same values of D_* at three different points in space. Time scales of the forward reaction τ_1 and the backward reaction τ_2 can be estimated as the times of rise and fall of the ferriin concentration. (g) The mean profile of the target waves for both diffusion coefficients estimated by averaging over all targets measured. (h) Different widths w_1 and w_2 of the profile in dependence of the diffusion coefficient D_*. The full width w_2 of the target wave grows with $\sqrt{D_*}$ as expected while the width of the rising edge w_1 stays constant.

Fig. 3(g) depicts the mean profiles of the boosted targets. These measurements were repeated for all turbulent diffusion coefficients [Fig. 3(h)]. While the full width w_2 of the boosted target waves increases according to $w_2 \propto \sqrt{D_*}$, as expected for an ideal reaction-diffusion system [23], the width of the rising edge w_1 does not change within the error of the measurement. A possible explanation for this unexpected behavior of w_1 is the intermittency of the mixing process. Averaging over many sharply defined filaments could give a similar width for the mean profile as the average over a smoother and broader front. This indicates that for low forcings and on the time scale τ_1 of the fast forward reaction occurring at the leading edge of the front [Fig. 3(f)], mixing might not yet be well defined by a diffusive process. According to this picture, w_2 augments diffusively as the backward reaction at the tail of the front is much slower with a time scale τ_2 [Fig. 3(f)] and sees a well developed diffusive process.

In summary, we conclude that complex spatiotemporal patterns, such as target and spiral waves, occur in turbulent fluid flows as was shown experimentally. Measuring turbulent diffusion coefficients and the reaction front velocities at various Reynolds numbers we find that they obey the FKPP relation for reaction-diffusion systems in contrast to what was found for similar large-scale patterns in a cellular flow [10]. The overall patterns resemble those of their molecular counterparts; however, an important difference is the filamentary appearance of the front which leads to an unexpected scaling of the front width. We suggest that this phenomenon can be understood by the existence of coherent structures in the flow that are known to exist in two-dimensional turbulent flows. We expect our results to increase the attention on pattern formation in systems where excitable dynamics evolve in turbulent flows, such as plankton growth in the ocean where a ring-like structure, similar to a target, has been reported [29,30].

This work was supported by the Ministerio de Educacion y Ciencia under Research Grants No. FIS2010-21023. A. v. K. and F. H. received funding from FPU, Grants No. AP-2009-0713 and No. AP-2009-3550. The authors want to thank Emilio Hernández García for stimulating discussions.

*Corresponding author.
alexandra.vonkameke@usc.es

[1] V. Smetacek *et al.*, Nature (London) **487**, 313 (2012).
[2] Z. Neufeld and E. Hernández-García, *Chemical and Biological Processes in Fluid Flows* (Imperial College Press, London, 2010).
[3] Y. Yu *et al.*, Nature (London) **109**, 2585 (2012).
[4] S. Luther *et al.*, Nature (London) **475**, 235 (2011).
[5] R. Kapral and K. Showalter, *Chemical Waves and Patterns* (Kluwer Academic Publishers, Dordrecht, 1995).
[6] V. Pérez-Muñuzuri, R. Aliev, B. Vasiev, Pérez-Villar, and V. I. Krinsky, Nature (London) **353**, 740 (1991).
[7] F. Huhn, A. von Kameke, V. Pérez-Muñuzuri, M. J. Olascoaga, and F. J. Beron-Vera, Geophys. Res. Lett. **39**, L06602 (2012).
[8] R. Grigoriev and H. G. Schuster, *Transport and Mixing in Laminar Flows* (Wiley-VCH, Berlin, 2011).

[9] P. D. Ronney, B. D. Haslam, and N. O. Rhys, Phys. Rev. Lett. **74**, 3804 (1995).
[10] J. R. Boehmer and T. H. Solomon, Europhys. Lett. **83**, 58 002 (2008).
[11] P. E. Arratia and J. P. Gollub, Phys. Rev. Lett. **96**, 024501 (2006).
[12] A. J. Majda and P. R. Kramer, Phys. Rep. **314**, 237 (1999).
[13] B. D. Haslam and P. D. Ronney, Phys. Fluids **7**, 1931 (1995).
[14] A. von Kameke, F. Huhn, G. Fernández-García, A. P. Muñuzuri, and V. Pérez-Muñuzuri, Phys. Rev. Lett. **107**, 074502 (2011).
[15] A. von Kameke, F. Huhn, G. Fernández-García, A. P. Muñuzuri, and V. Pérez-Muñuzuri, Phys. Rev. E **81**, 066211 (2010).
[16] See Supplemental Material at http://link.aps.org/supplemental/10.1103/PhysRevLett.110.088302 for methods summary, supplemental figures, and movies.
[17] K. Kurin-Csörgei, A. M. Zhabotinsky, M. Orbán, and I. R. Epstein, J. Phys. Chem. **100**, 5393 (1996).
[18] V. Pérez-Muñuzuri and F. Huhn, Nonlinear Proc. Geophys. **17**, 177 (2010).
[19] P. Foerster, S. C. Müller, and B. Hess, Proc. Natl. Acad. Sci. U.S.A. **86**, 6831 (1989).
[20] A. S. Mikhailov, *Foundations of Synergetics I: Distributed Active Systems* (Springer-Verlag, Heidelberg, 1990).
[21] A. S. Mikhailov and V. S. Zykov, in *Chemical Waves and Patterns*, edited by R. Kapral and K. Showalter (Kluwer Academic Publishers, Dordrecht, 1995).
[22] N. B. Tufillaro, R. Ramshankar, and J. P. Gollub, Phys. Rev. Lett. **62**, 422 (1989).
[23] J. D. Murray, *Mathematical Biology* (Springer-Verlag, Heidelberg, 1989).
[24] E. Mori, I. Schreiber, and J. Ross, J. Phys. Chem. **95**, 9359 (1991).
[25] L. Kuhnert, H.-J. Krug, and L. Pohlmann, J. Phys. Chem. **89**, 2022 (1985).
[26] A. Brandenburg, N. E. L. Haugen, and N. Babkovskaia, Phys. Rev. E **83**, 016304 (2011).
[27] G. Boffetta and R. E. Ecke, Annu. Rev. Fluid Mech. **44**, 427 (2012).
[28] C. R. Koudella and Z. Neufeld, Phys. Rev. E **70**, 026307 (2004).
[29] D. M. Dubois, Mem. Soc. R. Sci. Liege **VII**, 75 (1975).
[30] T. Wyatt, Marine biology **22**, 137 (1973).